JOURNAL OF GEOPHYSICAL RESEARCH, VOL. 114, D16113, doi:10.1029/2008JD011686, 2009

Harvesting model uncertainty for the simulation of interannual variability

Vasubandhu Misra[1]

Received 30 December 2008; revised 1 May 2009; accepted 11 June 2009; published 29 August 2009.

[1] An innovative modeling strategy is introduced to account for uncertainty in the convective parameterization (CP) scheme of a coupled ocean-atmosphere model. The methodology involves calling the CP scheme several times at every given time step of the model integration to pick the most probable convective state. Each call of the CP scheme is unique in that one of its critical parameter values (which is unobserved but required by the scheme) is chosen randomly over a given range. This methodology is tested with the relaxed Arakawa-Schubert CP scheme in the Center for Ocean-Land-Atmosphere Studies (COLA) coupled general circulation model (CGCM). Relative to the control COLA CGCM, this methodology shows improvement in the El Niño–Southern Oscillation simulation and the Indian summer monsoon precipitation variability.

Citation: Misra, V. (2009), Harvesting model uncertainty for the simulation of interannual variability, *J. Geophys. Res.*, *114*, D16113, doi:10.1029/2008JD011686.

1. Introduction

[2] Significant improvement in the simulation of variability at seasonal to interannual time scales by coupled ocean-atmosphere models has been accomplished over the years [*AchutaRao and Sperber*, 2006; *Saha et al.*, 2006; *Annamalai et al.*, 2007]. This has stemmed mostly from the improvement in the El Niño–Southern Oscillation (ENSO) simulation. Yet the challenges of prediction at seasonal to interannual time scales remain, especially with ENSO [*Goddard and DeWitt*, 2005; B. P. Kirtman and A. Pirani, WCRP seasonal prediction position paper, 2008, available at http://www.clivar.org/organization/wgsip/spw/spw_position.php]. For example, it is widely recognized that coupled models have the erroneous split Intertropical Convergence Zone (ITCZ) phenomenon: cold bias in the equatorial Pacific, warm bias in the subtropical eastern oceans, too diffuse a thermocline in the tropical latitudes, insufficient upwelling along the western boundaries of continents, and interannual variability that extends too far to the west in the equatorial Pacific [*de Szoeke and Xie*, 2008; *Misra et al.*, 2007; *Wittenberg et al.*, 2006; *Guilyardi*, 2006; *Mechoso et al.*, 1995].

[3] The motivation for this study stems from recent advances in addressing some of these issues by making relatively small changes to the convective parameterization (CP) scheme [*Bacmeister et al.*, 2006; *Zhang and Wang*, 2006; *Neale et al.*, 2008; *Zhang and Mu*, 2005]. *Bacmeister et al.* [2006] find that inclusion of rain evaporation helps lessen the double ITCZ problem. *Zhang and Wang* [2006] show that by modifying the closure of the *Zhang and McFarlane* [1995] convection scheme, the warm bias in the southern ITCZ and the cold bias in the cold tongue are significantly reduced. Similarly, *Neale et al.* [2008] find that inclusion of convective momentum transport and a dilution approximation for the calculation of convective available potential energy leads to significant improvements in the ENSO simulation. Therefore, there is ample evidence to suggest that the mean climate and its variability, at least at the seasonal to interannual time scales in a coupled general circulation model (CGCM), are sensitive to the CP scheme. It is this sensitivity that is being exploited in this study to harvest potential skill from the model.

[4] *Palmer* [2001], on the other hand, questioned the validity of the conventional parameterization schemes used in current climate models that make use of deterministic bulk formulae, which depend on resolved scale variables. *Palmer* [2001] argues that because of the underlying assumption of the parameterization schemes that subgrid-scale variability is a slave of the grid-scale variations, some of the model systematic errors have stubbornly resisted upgrades in resolution and parameterization complexity. *Lander and Hoskins* [1997] also point out that in nature the spectrum of motions has no clear gap, and in fact any existent separation of scales becomes even narrower on scales of hundreds of kilometers or less (typical climate model resolution). Using low-order dynamical systems, *Palmer* [2001] showed that nonlocal dynamically based stochastic parameterization schemes that take into account variability of the subgrid scales result in major changes and improvements even on climate time scales. The European Centre for Medium-Range Weather Forecasts now uses a similar form of stochastic forcing in its operational weather and climate prediction model [*Palmer et al.*, 2005]. In other related work, *Rodwell and Palmer* [2007] and *Murphy et al.* [2004] showed that much of the perceived model uncertainty stems from the "fast physics" that isolates convection

[1]Department of Meteorology and Center for Ocean-Atmospheric Prediction Studies, Florida State University, Tallahassee, Florida, USA.

0148-0227/09/2008JD011686$09.00

Table 1. A Brief Outline of the COLA AGCM V3.2

Feature	Reference
Convection	*Moorthi and Suarez* [1992] and J. T. Bacmeister (unpublished manuscript, 2005)
Planetary boundary layer	*Hong and Pan* [1996]
Radiation	*Collins et al.* [2006]
Land surface	*Xue et al.* [1996] and *Dirmeyer and Zeng* [1999]
Diagnostic clouds and optical properties	*Kiehl et al.* [1998]

as one of the main sources of such uncertainty. It is therefore quite obvious that the cumulus parameterization scheme would be one of the natural choices for conducting model experiments on model uncertainty. The methodology is explained in section 3 after the model description is explained in section 2.

2. Model Description

[5] The Center for Ocean-Land-Atmosphere Studies (COLA) coupled climate model [*Misra et al.*, 2007; *Misra and Marx*, 2007] is used in this study. A brief outline of the COLA atmospheric general circulation model (AGCM) is provided in Table 1. Similarly, a brief outline of the ocean general circulation model (OGCM) [*Pacanowski and Griffies*, 1998] is provided in Table 2. The COLA AGCM is run at T62 spectral truncation with 28 sigma levels. The OGCM has a uniform zonal resolution of 1.5°, while the meridional resolution is 0.5° between 10°S and 10°N, gradually increases to 1.5° at 30°N and 30°S, and is fixed at 1.5° in the extratropics.

3. Methodology

[6] The CP scheme implemented in the COLA coupled climate model is the relaxed Arakawa-Schubert (RAS) scheme [Moorthi and Suarez 1992; J. T. Bacmeister, Moist processes in the GEOS5 AGCM, 2005, available at http://gmao.gsfc.nasa.gov/systems/geos5/STRUCTURE/AGCM/Moist.php]. There is no explicit downdraft in this implementation. In this scheme, a fraction of the convective condensate is shielded from rain evaporation that is meant to represent falling through a saturated environment (as in saturated downdraft). Without appropriate representation of the convective rain evaporation, *Nitta* [1978] inferred that excessive subsidence and drying in the surrounding environment is likely to occur. *Sud and Molod* [1988] and *Sud and Walker* [1993] showed that inclusion of rain evaporation had a significant impact on improving the simulation of the tropical environment. *Maloney and Hartmann* [2001] indicated that convective reevaporation may also help in preconditioning the tropical atmosphere for deep Madden-Julian oscillation convection.

[7] In the *Sud and Molod* [1988] convective rain reevaporation scheme, the reevaportation occurs after each cloud type has relaxed the environmental sounding toward quasi-equilibrium. In this way they ensure that the subsequent cloud types feel the environmental moistening from evaporation. However, in the methodology proposed by *Moorthi* [2000] and J. T. Bacmeister (unpublished manuscript, 2005) each cloud type (determined uniquely by the detrainment level) within a given call to the RAS scheme does not recognize the moistening from convective reevaporation from the previous cloud type and itself until the next time step of the model integration. Following *Moorthi* [2000] and J. T. Bacmeister (unpublished manuscript, 2005) the rain evaporation at and below the level of available convective condensate is given by

$$R_f = \min\left\{1, \frac{\Delta q}{P}\sigma\left[P(3600/\Delta t)(p/1000)^{0.5}\right]^{0.578}\right\},$$

where Δq is the saturation moisture deficit, P is available convective condensate for reevaporation, p is midlevel pressure of the layer where reevaporation is occurring, and σ is the horizontal fractional area covered by the falling precipitation, which is given by

$$\sigma = \min\{1, \eta g M_B N_T/\Delta p_i\}.$$

Here, M_B is cloud base mass flux, N_T is the normalized mass flux at cloud top, Δp_i is the pressure thickness of the layer, and η is an empirical parameter. A similar rain evaporation scheme (as above) is implemented in the National Aeronautics and Space Agency (NASA) Goddard Earth Observing System Model version 5 (GEOS-5) [*Rienecker et al.*, 2008].

[8] The unobserved parameter η is defined to represent evaporation efficiency that can be modified empirically. However, it is meant to represent the shear-dependent parameters that control the shielded fraction of the convective rain, as well as the relationship between the diagnosed updraft areal fraction and convective shower area. It is this parameter η (convective rain evaporation efficiency) that is modulated in the proposed methodology. *Bacmeister et al.* [2006] found that the choice of this parameter has a tremendous implication for the mean tropical climate. They found that increasing the convective rain evaporation entailed the prevention of the feedback between convective heating and planetary boundary layer convergence in high-frequency modes. This in turn resulted in the reduction of the split ITCZ phenomenon in the eastern Pacific during the boreal summer season. Therefore, η is an obvious choice for accounting for its uncertainty as it is empirical and has a potentially significant impact on the mean climate of the CGCM.

[9] The idea is to provide one unique estimate of convective heating, moistening, and condensate rate (collectively referred to as convective state) based on a robust estimate of η. This is accomplished by calling the part of the CP scheme that deals with the rain evaporation several times per time step of the AGCM, each time with a unique

Table 2. A Brief Outline of the OGCM of the COLA Coupled Model[a]

Feature	Reference
Vertical mixing	*Large et al.* [1994]
Momentum mixing	*Smagorinsky* [1963]
Tracer mixing	*Redi* [1982]
Quasi adiabatic stirring	*Gent and McWilliams* [1990]

[a]The OGCM used was MOM3.0.

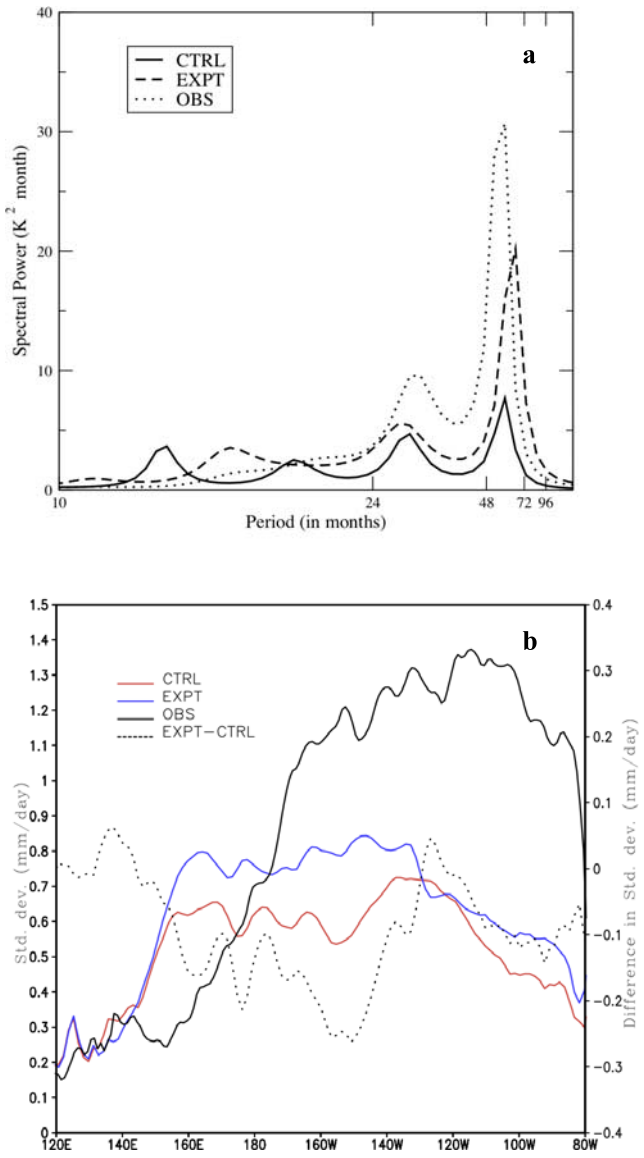

Figure 1. (a) The maximum entropy spectra of Niño3 SST and (b) standard deviation of equatorial SST from the EXPT and CTRL, their differences, and the corresponding observations.

value of η. This does not prove to be computationally cumbersome because the methodology is adopted only at those grid points which have nonzero convective rain. Furthermore, evaporation of the convective rain in the implemented RAS scheme is performed last, after accumulating the convective condensate from all the RAS plumes.

[10] The methodology is explained with the illustration and is followed by the experimental model integration (hereinafter referred as EXPT). The methodology is also described in Appendix A and illustrated Figure A1 in the form of a flowchart. One hundred calls to the convective rain evaporation part of the CP scheme are made, each with unique values of η, at every time step of the AGCM. Some preliminary model integrations for a period of 10 years (not shown) were made for 10, 20, 80, and 100 calls of the evaporation part of the CP scheme. It was observed that the differences in the mean tropical Pacific sea surface temperature (SST) and the zonal mean precipitation distribution and its variability between the 100 and the 80 call experiments were significantly smaller than those for the 10 and 20 call experiment. This suggested a convergence of the model solutions at least over the tropics at the higher calls to the evaporation part of the CP scheme. Therefore, the choice of 100 calls was made on the basis of these preliminary experiments. It is, however, admittedly an ad hoc method, which requires further investigation in the future. These 100 values of η are picked randomly over a given range, which is chosen a priori to be between 0.01 and 0.2 (while in the control (CTRL) model it is fixed at 0.1). Corresponding to each η, there is a surface precipitation flux with associated heating and moistening rates. These fluxes of precipitation are sorted and ordered in an ascending order. The series is then divided, for example, into 10 unequal bins (or clusters), such that each bin has an equal number of members (which in this case will be 10 deciles). The bin (or cluster) with the least spread of the precipitation flux is isolated. Then the η parameter corresponding to a random choice of precipitation within the isolated bin with the least spread is assigned the most probable value. A random choice in the bin with the least spread is made in order to recognize that the most probable value is being estimated from a finite sample size. The selection of precipitation as a metric for this procedure, apart from being a convenient and a natural choice, also stems from the insensitivity of replacing it with cloud work function. The proposed methodology in this paper is somewhat akin to the random modulation of the vertical distribution of convective heating adopted by *Lin and Neelin* [2002].

[11] The proposed methodology is a form of a clustering technique. The physical basis of the methodology follows from the following argument: if the convective event is parameterizable, i.e., the subgrid-scale precipitation is a robust function of the large scale, then minor changes to the tuning parameters of the convection scheme should ideally yield a cluster with a relatively small dispersion (or intraensemble difference). In other words, the large scale and not the choice of η (in this case) will largely dictate the resulting convective state in a parameterizable event. If the convective event is, however, not parameterizable, then the event is random. Therefore, any value of η that the clustering technique isolates for a nonparameterizable convective event is reasonable (as all values of η are equally probable).

4. Results

[12] The model integrations conducted in this study were performed for 70 years. But the results are presented from the last 50 years of the integration. The CTRL integration is conducted with the COLA coupled model version 3.2 [*Misra et al.*, 2007]. The coupled mean state of the model was well spun up before the start of the integration [*Misra and Marx*, 2007].

4.1. Niño3 SST Spectrum

[13] As mentioned in section 1, many recent studies have shown significant sensitivity regarding large-scale features, such as the ENSO simulation in a coupled ocean-atmosphere model to the convective parameterization scheme. ENSO

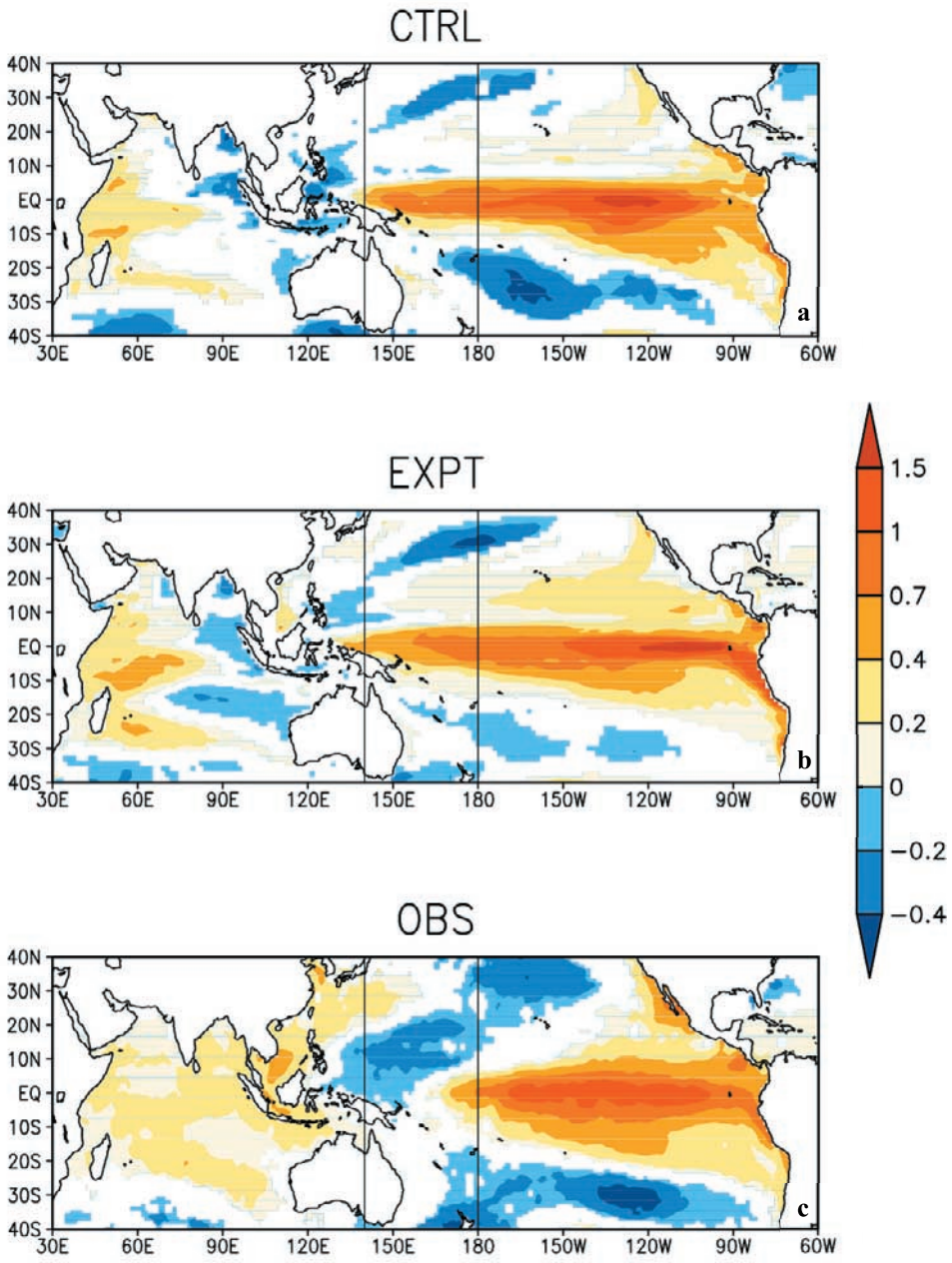

Figure 2. The regression of the tropical Pacific SST anomalies on the Niño3 SST anomalies from the (a) CTRL and (b) EXPT model simulations and (c) OBS (HADISST1.1). The units are in °C. Only significant values at 90% confidence according to the *t* test are shaded.

has a characteristic broad spectral peak in the range of 2–7 years in the Niño3 SST spectrum. This feature has often been used to assess the ENSO simulation in coupled climate models [*Meehl and Arblaster*, 1998; *AchutaRao and Sperber*, 2006]. In Figure 1a, we show the Niño3 SST spectrum using the maximum entropy method of *Ghil et al.* [2002] from the CTRL and the EXPT integrations along with the observations (Hadley Centre Global Sea Ice and Sea Surface Temperature version 1.1 (HADISST)) [*Rayner et al.*, 2003]. The EXPT shows some improvement in the amplitude of the ENSO events relative to the CTRL. Furthermore, the period of the peak variability is shifted slightly to a longer period of around 5 years relative to about 4 years in the CTRL and observations.

[14] The standard deviation of the annual mean SST along the equator shown in Figure 1b is consistent with the spectrum shown in Figure 1a. The EXPT shows higher variability over the central and eastern equatorial Pacific Ocean. However, both model integrations underestimate the variance over the central and eastern equatorial Pacific Ocean compared to the observations. Furthermore, both models erroneously produce more variance over the western Pacific Ocean (west of the date line) compared to the observations. It will be shown in section 4.2 that the excessive variance west of the date line in EXPT seems to

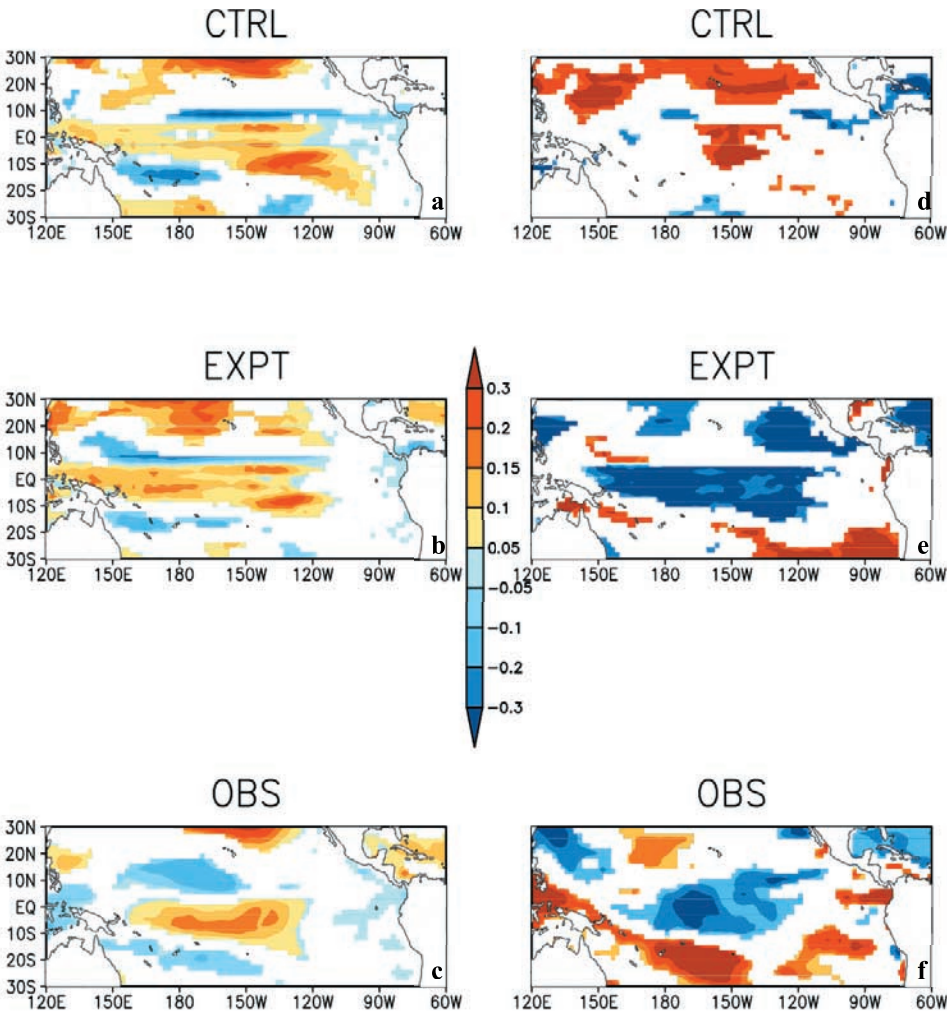

Figure 3. The regression of the annual mean tropical Pacific zonal wind stress anomalies on the annual mean Niño3 SST anomalies from the (a) CTRL and (b) EXPT model simulations and (c) OBS (NCEP-NCAR reanalysis wind stress and HADISST1.1). The regression of the DJF mean tropical zonal wind stress anomalies on the preceding Indian monsoon rainfall from the (d) CTRL and (e) EXPT simulations and (f) OBS (NCEP-NCAR reanalysis wind stress and precipitation). The units are in dyn cm^{-2}. Only significant values at 90% confidence according to the *t* test are shaded.

be less related to variations of the SST in Niño3 region compared to the CTRL. However, this excessive variation of SST in the western equatorial Pacific region in the EXPT may be considered as one of the deteriorations from the CTRL.

4.2. ENSO-Related SST Variations

[15] In Figure 2, the contemporaneous regression of the Niño3 SST anomalies on the global tropical SST anomalies is displayed. The peak SST variability is shifted eastward in the EXPT relative to both the observations and the CTRL. A marginal improvement in the EXPT relative to the CTRL is observed in the reduction of the westward extension of the SST variance in the western equatorial Pacific Ocean that is related to the Niño3 SST index variations between the longitudes of 140°E and the date line. Additionally, the EXPT (Figure 2a) shows increased variability of SST in the far east Pacific along the coast of Peru, while the CTRL (Figure 2b) underestimates the variance relative to the observations (Figure 2c).

4.3. Indian Monsoon ENSO Teleconnection

[16] A number of studies in the past have suggested that the Indian monsoon can impact the ENSO evolution [*Barnett*, 1984; *Webster and Yang*, 1992; *Kirtman and Shukla*, 2000; *Wu and Kirtman*, 2006]. *Kirtman and Shukla* [2000] showed that the monsoon heating modulates the Walker circulation, which results in anomalies of the trade winds in the Pacific Ocean. These trade wind anomalies in turn change the wind stress forcing on the ocean, which then has a bearing on the evolution of the ocean currents, thermocline depth, SST, and the heat fluxes. In this study we show some evidence of a similar behavior, which helps in understanding the difference of the ENSO simulation in the EXPT and the CTRL integrations.

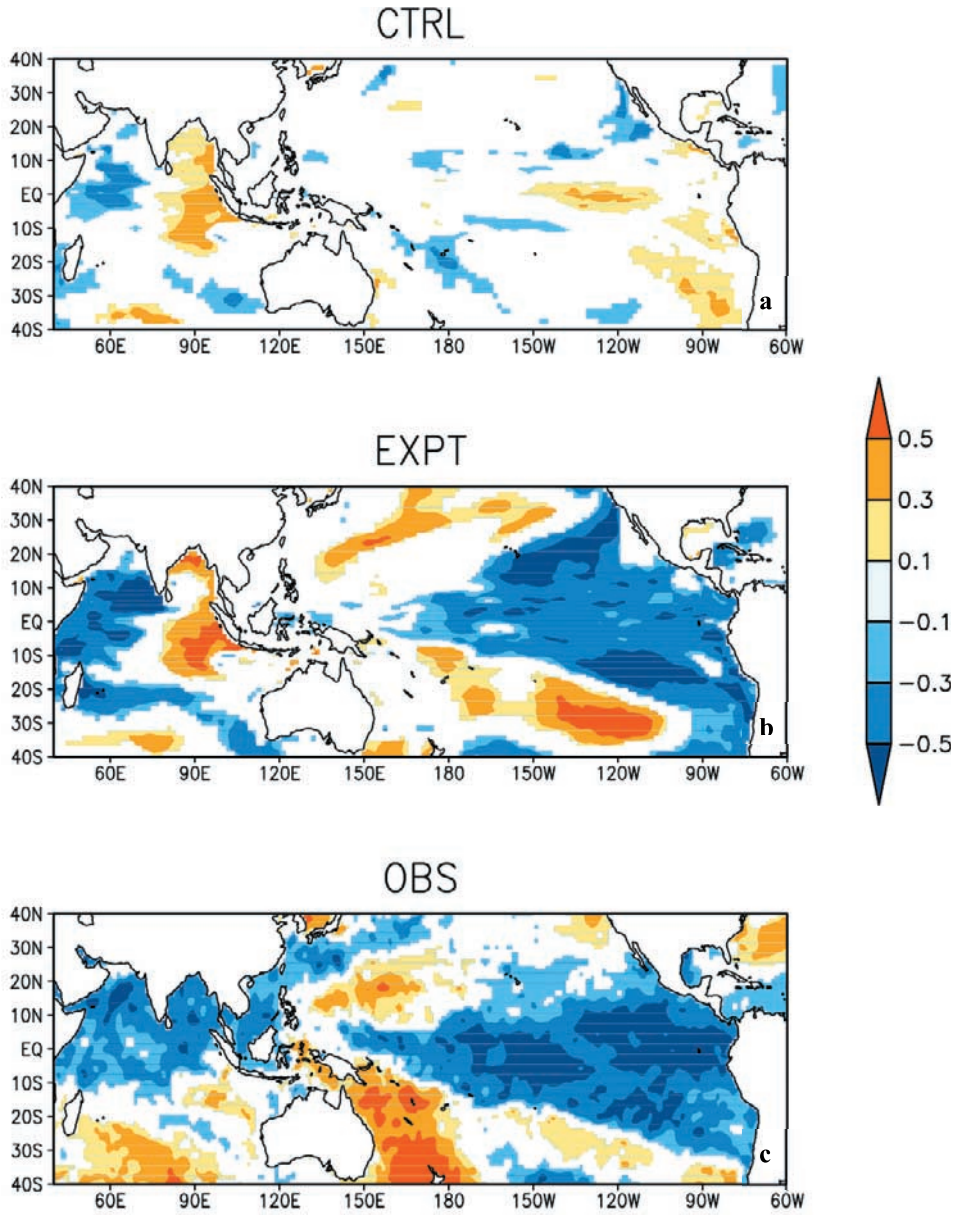

Figure 4. The regression of the DJF mean tropical Pacific SST anomalies on the preceding JJAS mean IMR index from the (a) CTRL and (b) EXPT model simulations and (c) OBS (rainfall from *Rajeevan et al.* [2006] and HADISST1.1). The units are in °C. Only significant values at 90% confidence according to the *t* test are shaded.

[17] In Figures 3a–3c we show the contemporaneous regression of the annual mean tropical Pacific wind stress anomalies on the Niño3 SST index from the CTRL, EXPT, and observations (OBS) (National Centers for Environmental Prediction (NCEP)–National Center for Atmospheric Research (NCAR) reanalysis [*Kalnay et al.*, 1996] wind stress with HADISST). All of them show significant wind stress anomalies in the western and central equatorial Pacific Ocean straddled by anomalies of opposite sign in either hemisphere. This relationship suggests the Bjerknes feedback mechanism [*Bjerknes*, 1969], which relates thermocline variability from equatorial upwelling anomalies as a response to wind stress anomalies. The wind stress anomalies in the CTRL (Figure 3a) are weaker and eastward relative to either the EXPT (Figure 3b) or the OBS (Figure 3c). This wind stress anomaly is, however, strongly correlated with the Indian monsoon rainfall (IMR) anomalies. This is shown in Figures 3d–3f. Here, the December-January-February (DJF) zonal wind stress anomaly is regressed with the preceding June-July-August-September (JJAS) IMR index, which is defined as all land points between 5°N and 28°N and between 60°E and 100°E [*Parthasarathy et al.*, 1994]. The zonal wind stress anomalies in the EXPT (Figure 3e) and in the NCEP reanalysis (Figure 3f) closely resemble the ENSO-related anomalies in Figures 3b and 3c, respectively. However, the CTRL model in Figure 3d shows a poor teleconnection with its IMR index. In other words, in both the EXPT and the NCEP-

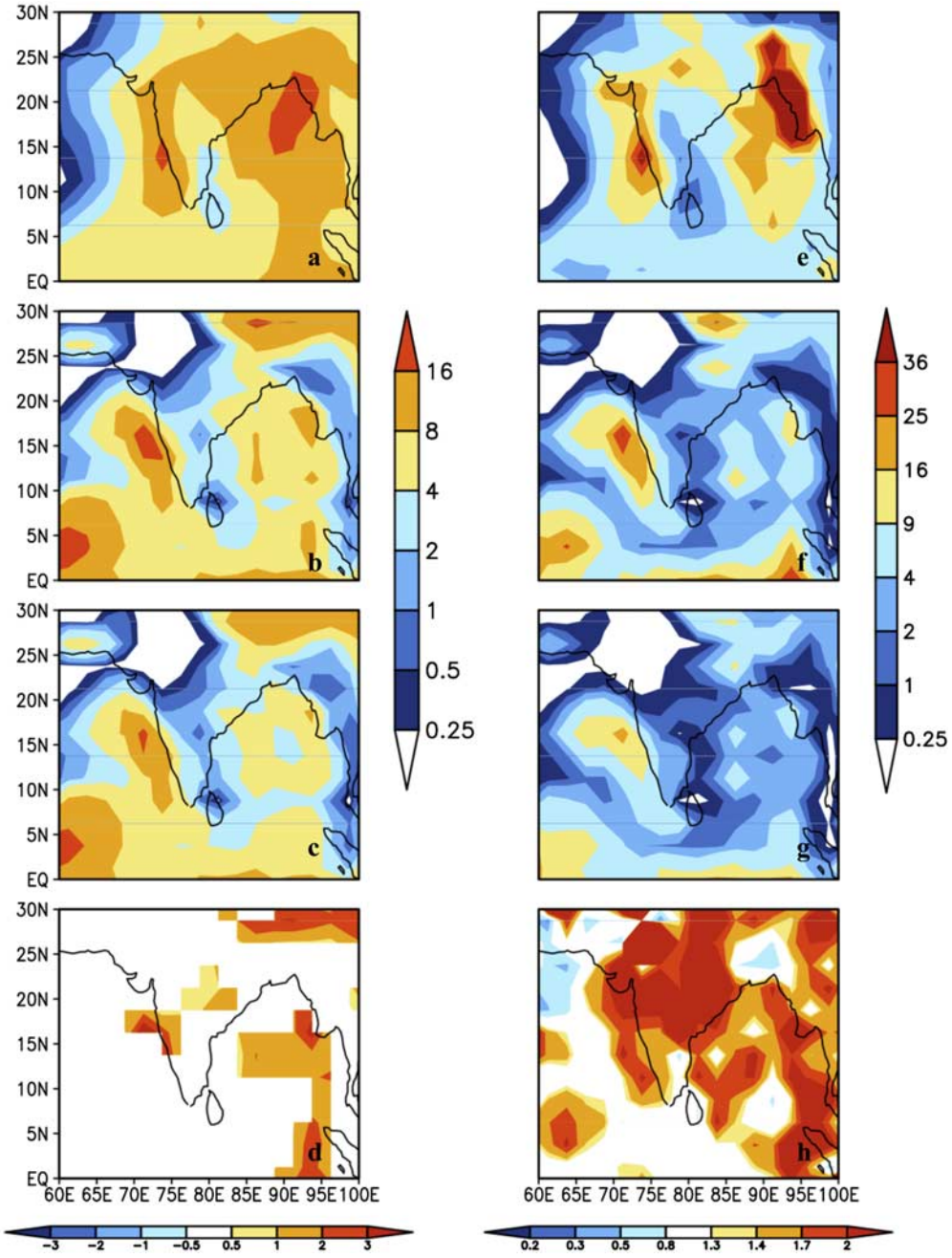

Figure 5. The climatological mean JJAS precipitation (mm d^{-1}) from (a) observations [*Xie and Arkin*, 1996], (b) EXPT simulations, and (c) the CTRL simulation. (d) The climatological mean JJAS precipitation difference (mm d^{-1}) between EXPT and CTRL simulations. Only significant values at the 90% confidence interval according to *t* test are plotted. The corresponding variance of the mean JJAS precipitation (mm^2 d^{-2}) from (e) observations, (f) EXPT simulations, and (g) the CTRL simulation. (h) The ratio of the variance of the mean JJAS precipitation between EXPT and CTRL. Only significant values at 90% confidence according to the *F* test are shaded.

NCAR reanalysis, the zonal wind stress anomalies in the equatorial Pacific are a strong function of the preceding Indian monsoon. In a similar vein, *Kirtman and Shukla* [2000] in their diagnostic modeling study showed that the Indian monsoon variability modulates the strength of the trade winds in the equatorial Pacific.

[18] The IMR teleconnection with the tropical Pacific SST at interannual time scales is one of the most difficult to capture in a coupled ocean-atmosphere model [*Kirtman and Shukla*, 2002]. In Figures 4a and 4b, the regression of the DJF mean tropical Pacific SST on the preceding JJAS mean IMR index of the CTRL and EXPT model runs are shown, respectively. The corresponding observations are displayed in Figure 4c. There is a dramatic difference in this teleconnection pattern between the model simulations, with the EXPT conforming more to the observations. The tele-

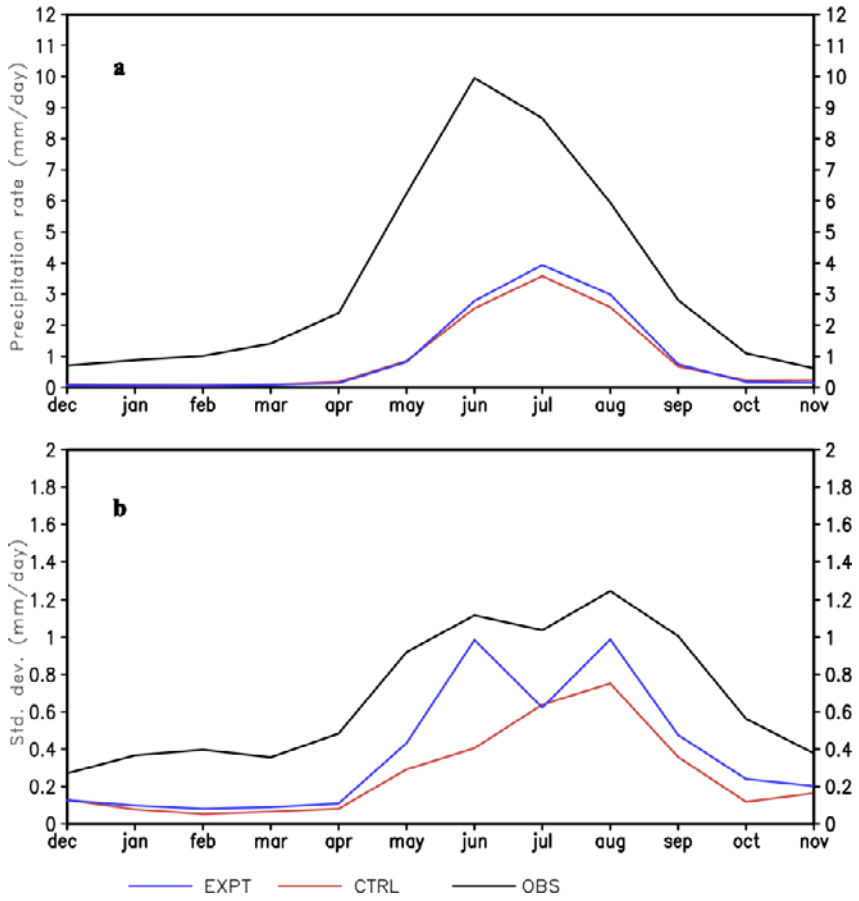

Figure 6. (a) The annual cycle of the IMR index (see text for definition) and (b) the annual cycle of the standard deviation of the IMR index.

connection pattern in the CTRL suggests that a strong (weak) Indian monsoon precedes a warm (cold) ENSO event, which is contrary to the observations.

4.4. Indian Monsoon

[19] In Figures 5a–5c we show the mean JJAS rainfall over the Indian monsoon region from observations (Climate Prediction Center Merged Analysis Precipitation (CMAP)) [*Xie and Arkin*, 1996], the EXPT and the CTRL simulations. The EXPT integration is able to capture the seasonal maximum along the Arabian Sea coast and over the Bay of Bengal with a minimum over Sri Lanka and along the east coast of India, albeit the magnitude of the variance over these regions is off compared to the observations. The EXPT simulation also underestimates (overestimates) the mean rainfall over central and northwest India, the Bay of Bengal, and Sri Lanka (Arabian Sea) quite significantly. The CTRL shows a similar bias (Figure 5c) as the EXPT. The corresponding climatological mean JJAS difference between the EXPT and the CTRL is shown in Figure 5d. Despite the dry bias over central India, the EXPT simulation is a slight improvement relative to the CTRL over central India. Similarly, the corresponding variance of the seasonal mean JJAS rainfall is also underestimated in the EXPT integration (Figure 5f) relative to the observations (Figure 5e), especially over the Bay of Bengal and central India. However, the variance of the JJAS seasonal rainfall in EXPT is a significant improvement over the underestimated variance in the CTRL (Figures 5g and 5h), particularly over the Indian subcontinent.

[20] In terms of the phase of the seasonal cycle of the IMR index, both the EXPT and the CTRL seem to be in reasonable agreement with the observations (CMAP, Figure 6a). However, the magnitude of the monthly rainfall is underestimated throughout the year, with larger differences in the boreal summer monsoon season. The corresponding seasonal cycle of the standard deviation of the IMR index is shown in Figure 6b. Here, the EXPT as in Figure 5h shows significant improvement over the CTRL, in terms of both its magnitude and its phase.

4.5. Intraseasonal Variability

[21] The observed intraseasonal (10–100 days) variance of the National Oceanic and Atmospheric Administration (NOAA) outgoing longwave radiation (OLR) [*Liebmann and Smith*, 1996] in the boreal summer (JJAS) and winter (November-December-January-February (NDJF)) is shown in Figures 7a and 7e. The OLR is filtered using a fourth-order Butterworth filter. The latitudinal shift of the large intraseasonal variance of OLR from the domain of the Indian monsoon in the boreal summer season to over northern Australia in the boreal winter is quite apparent.

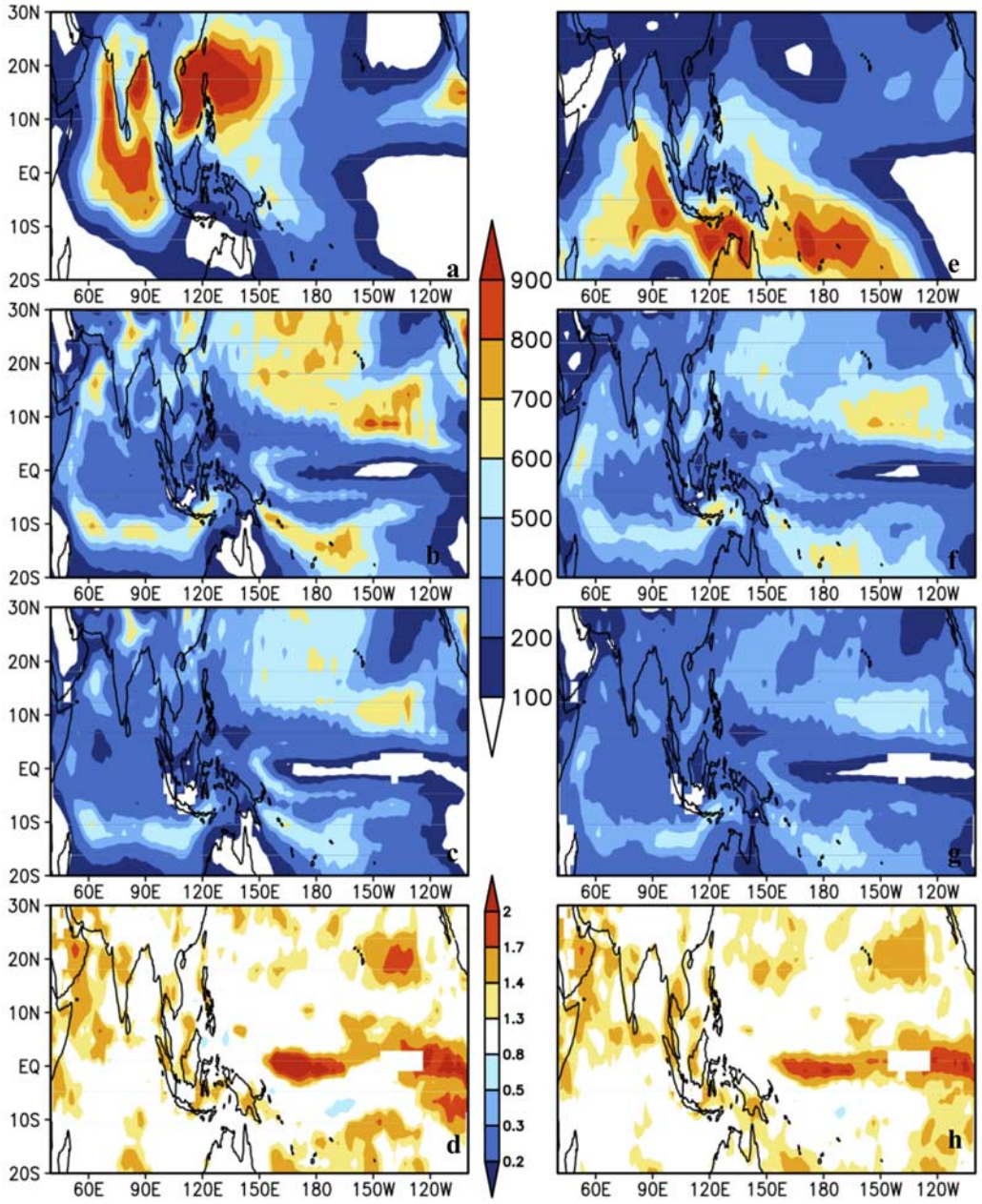

Figure 7. The mean intraseasonal variance (10–100 days) of OLR in boreal summer season (JJAS) from (a) observations, (b) EXPT simulation, and (c) the CTRL simulation. (d) The ratio of the intraseasonal variance in the boreal summer season between the EXPT and CTRL simulations. (e, f, and g) Similar to Figures 7a, 7b, and 7c but for boreal winter season (NDJF). The units are in $W^2\ m^{-4}$. (h) Similar to Figure 7d but for boreal winter season. Only significant values at the 90% confidence interval according to the *F* test are shaded in Figures 7d and 7h.

The corresponding simulation of the intraseasonal variance of OLR in the EXPT simulation in Figures 7b and 7f is rather poor. The intraseasonal variance is underestimated over the tropical Indian Ocean and the western Pacific Ocean in the EXPT simulation. Furthermore, the intraseasonal variance in the EXPT simulation is, erroneously, more a standing oscillation in the tropical oceans (not shown, but also evident from the absence of the seasonal shift in Figures 7b and 7f). The CTRL (Figures 7c and 7g) shows far less intraseasonal variance than the EXPT. But the patterns of the intraseasonal variance are comparable in the two model integrations.

5. Conclusions

[22] A new modeling strategy was presented in this work in order to make the solutions from a climate model relatively less dependent on the unobserved empirical parameters of the parameterization scheme. On the basis of a variety of reasons, including some past studies on the

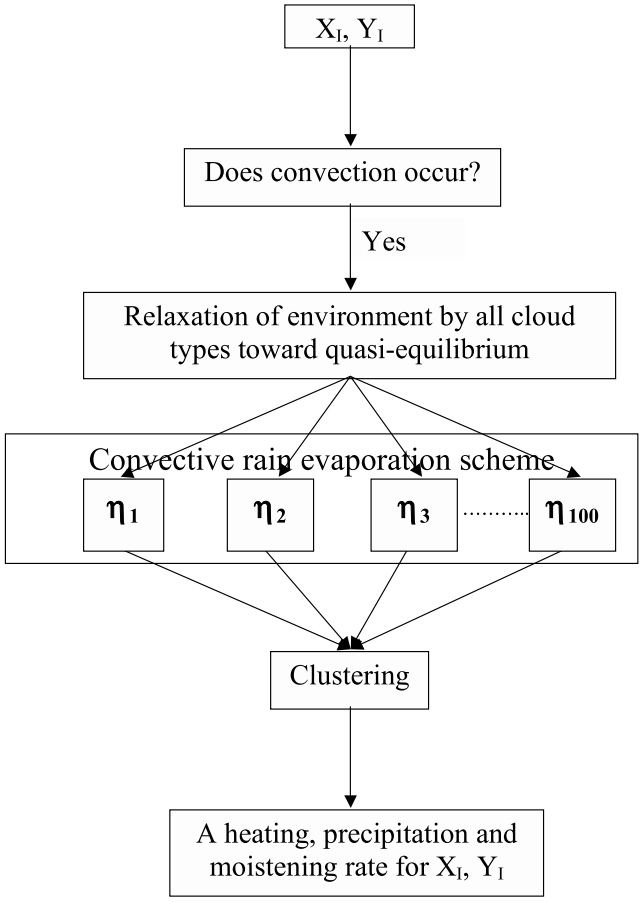

Figure A1. The methodology described in the main text is shown as a flow chart in Figure A1.

sensitivity of climate simulations to the cumulus parameterization (CP) scheme, the strategy entailed getting a robust estimate of the atmospheric convective state at every time step of the model integration. This methodology has the advantage of being able to run on computing resources comparable to those of the CTRL model, which is otherwise strained by even moderate increases in the spatial resolution of the model.

[23] This study shows that adopting this strategy in the model results in some benefits to improving the ENSO simulation, and the mechanism for this improvement is conjectured to come from the remote forcing of the Indian monsoon on the zonal wind stress anomalies over the equatorial Pacific Ocean. However, the simulation of the intraseasonal variance of OLR is disappointing in the EXPT simulation with underestimation of the variance and absence of significant eastward (meridional) propagation in the boreal winter (summer) season. It should be mentioned that the premise of estimating η from the proposed methodology is akin to raising parameter resolution. It is somewhat gratifying to note that the mean state of the Indian monsoon does not change significantly between the EXPT and the CTRL. This attests to the fact that the mean Indian summer monsoon is not critically dependent on the choice of the unobserved empirical parameter η at least in the COLA coupled climate model [*Misra et al.*, 2007]. However, we have shown that the tropical variability of ENSO and the Indian monsoon are quite robustly modulated in the same climate model, indicating that the proposed methodology has merit in harvesting the model uncertainty for predictability at seasonal to interannual time scales. Furthermore, unlike other multimodel strategies where model results are combined a posteriori, violating conservation laws, the proposed methodology is consistent with the model equations, and is thus amenable to thorough diagnostic studies.

[24] There is, however, scope for further development of this scheme, especially in exploring other empirical parameters in other physical parameterization schemes. While seeking higher spatial resolutions of these climate models is possibly a valid pursuit of scientific research, this study shows that there could be some benefit to reap from providing resolution to parameter estimation in general circulation models.

Appendix A

[25] As described in the main text and illustrated here in Figure A1, the methodology involves as a first step checking if convection (in this case the RAS scheme) is occurring at a given grid point X_I, Y_I of the AGCM. Should convection be active at X_I, Y_I, then RAS relaxes the environment by all cloud types toward quasi-equilibrium. The rain evaporation in RAS occurs at the end, after all the convective condensate from all the clouds is collected. The methodology takes advantage of this, to be able to call the rain evaporation part of the RAS scheme 100 times at every time step of the AGCM, each with a unique value of the rain evaporation efficiency parameter (η; η_1, η_2,. . .,η_{100}). The methodology to generate the values for η is explained in section 3. Then we adopt a clustering technique (explained in section 3) to isolate a unique and robust estimate of convective, moistening, and precipitation rates from these 100 realizations for the grid point X_I, Y_I.

[26] **Acknowledgments.** I thank my colleagues in the Department of Meteorology who gave their candid opinion on the paper when it was presented in the faculty happy hour (initiated by Xiaolei Zou). I also thank Ben Kirtman of RSMAS and two anonymous reviewers for their useful comments. In addition, the generous support of the Council on Research and Creativity (CRC) First Year Assistant Professor (FYAP) of FSU is appreciated. I would like to acknowledge the expert guidance of Meredith Field of COAPS for her editorial corrections on a couple of earlier versions of the manuscript and her help in creating the flowchart. The support from NOAA grant NA07OAR4310221 is acknowledged.

References

AchutaRao, K., and K. Sperber (2006), ENSO simulation in coupled ocean-atmosphere models: Are the current models better?, *Clim. Dyn.*, *27*, 1–15.

Annamalai, H., K. Hamilton, and K. R. Sperber (2007), The south Asian summer monsoon and its relationship with ENSO in the IPCC AR4 simulations, *J. Clim.*, *20*, 1071–1092, doi:10.1175/JCLI4035.1.

Bacmeister, J. T., M. J. Suarez, and F. R. Robertson (2006), Rain reevaporation, boundary layer–convection interactions, and Pacific rainfall patterns in an AGCM, *J. Atmos. Sci.*, *63*, 3383–3403, doi:10.1175/JAS3791.1.

Barnett, T. P. (1984), Interaction of the monsoon and Pacific trade wind system at interannual time scales. Part III: A partial anatomy of the southern oscillation, *Mon. Weather Rev.*, *112*, 2388–2400, doi:10.1175/1520-0493(1984)112<2388:IOTMAP>2.0.CO;2.

Bjerknes, J. (1969), Atmospheric teleconnections from the equatorial Pacific, *Mon. Weather Rev.*, *97*, 163–172, doi:10.1175/1520-0493(1969)097<0163:ATFTEP>2.3.CO;2.

Collins, W. D., et al. (2006), The Community Climate System Model Version 3 (CCSM3), *J. Clim.*, *19*, 2122–2143, doi:10.1175/JCLI3761.1.

de Szoeke, S. P., and S.-P. Xie (2008), The tropical eastern Pacific seasonal cycle: Assessment of errors and mechanisms in IPCC AR4 coupled ocean-atmosphere general circulation models, *J. Clim.*, *21*, 2573–2590, doi:10.1175/2007JCLI1975.1.

Dirmeyer, P. A., and F. J. Zeng (1999), Precipitation infiltration in the simplified SiB land surface scheme, *J. Meteorol. Soc. Jpn.*, *78*, 291–303.

Gent, P. R., and J. C. McWilliams (1990), Isopycnal mixing in ocean circulation models, *J. Phys. Oceanogr.*, *20*, 150–155, doi:10.1175/1520-0485(1990)020<0150:IMIOCM>2.0.CO;2.

Ghil, A., et al. (2002), Advanced spectral methods for climatic time series, *Rev. Geophys.*, *40*(1), 1003, doi:10.1029/2000RG000092.

Goddard, L., and D. DeWitt (2005), Seeking progress in El Niño prediction, *U.S. CLIVAR Variations 3*(1), 7 pp., U.S. Clim. Variability and Predictability Res. Prog., Washington, D. C.

Guilyardi, E. (2006), El Niño mean state-seasonal cycle interactions in a multi-model ensemble, *Clim. Dyn.*, *26*, 329–348, doi:10.1007/s00382-005-0084-6.

Hong, S. Y., and H. L. Pan (1996), Nonlocal boundary layer vertical diffusion in a medium range forecast model, *Mon. Weather Rev.*, *124*, 2322–2339, doi:10.1175/1520-0493(1996)124<2322:NBLVDI>2.0.CO;2.

Kalnay, E., et al. (1996), The NMC/NCAR 40-year reanalysis project, *Bull. Am. Meteorol. Soc.*, *77*, 437–471, doi:10.1175/1520-0477(1996)077<0437:TNYRP>2.0.CO;2.

Kiehl, J. T., J. J. Hack, G. Bonan, B. A. Boville, D. L. Williamson, and P. J. Rasch (1998), The National Center for Atmospheric Research Community Climate Model: CCM3, *J. Clim.*, *11*, 1131–1149, doi:10.1175/1520-0442(1998)011<1131:TNCFAR>2.0.CO;2.

Kirtman, B. P., and J. Shukla (2000), Influence of the Indian summer monsoon on ENSO, *Q. J. R. Meteorol. Soc.*, *126*, 213–239.

Kirtman, B. P., and J. Shukla (2002), Interactive coupled ensemble: A new coupling strategy for CGCMs, *Geophys. Res. Lett.*, *29*(10), 1367, doi:10.1029/2002GL014834.

Lander, J., and B. J. Hoskins (1997), Believable scales and parameterizations in a spectral transform model, *Mon. Weather Rev.*, *125*, 292–303, doi:10.1175/1520-0493(1997)125<0292:BSAPIA>2.0.CO;2.

Large, W. G., J. C. McWilliams, and S. C. Doney (1994), Oceanic vertical mixing: A review and a model with a nonlocal boundary layer parameterization project, *Clim. Dyn.*, *18*, 255–272.

Liebmann, B., and C. A. Smith (1996), Description of a complete (interpolated) outgoing longwave radiation dataset, *Bull. Am. Meteorol. Soc.*, *77*, 1275–1277.

Lin, J. W.-B., and J. D. Neelin (2002), Considerations for stochastic convective parameterization, *J. Atmos. Sci.*, *59*, 959–975, doi:10.1175/1520-0469(2002)059<0959:CFSCP>2.0.CO;2.

Maloney, E., and D. Hartmann (2001), The sensitivity of intraseasonal variability in the NCAR CCM3 to changes in convective parameterization, *J. Atmos. Sci.*, *14*, 2015–2034.

Mechoso, C. R., et al. (1995), The seasonal cycle over the tropical Pacific in coupled ocean-atmosphere general circulation models, *Mon. Weather Rev.*, *123*, 2825–2838, doi:10.1175/1520-0493(1995)123<2825:TSCOTT>2.0.CO;2.

Meehl, G. A., and J. M. Arblaster (1998), The Asian-Australian monsoon and El Niño Oscillation in the NCAR climate system model, *J. Clim.*, *11*, 1356–1385, doi:10.1175/1520-0442(1998)011<1356:TAAMAE>2.0.CO;2.

Misra, V., and L. Marx (2007), Manifestation of remote response over the equatorial Pacific in a climate model, *J. Geophys. Res.*, *112*, D20105, doi:10.1029/2007JD008597.

Misra, V., et al. (2007), Validating and understanding ENSO simulation in two coupled climate models, *Tellus, Ser. A*, *59*, 292–308.

Moorthi, S. (2000), Application of relaxed Arakawa-Schubert cumulus parameterization to the NCEP climate model: Some sensitivity experiments, in *General Circulation Model Development: Past, Present and Future*, edited by D. A. Randall, pp. 257–284, Academic, Orlando, Fla.

Moorthi, S., and M. J. Suarez (1992), Relaxed Arakawa-Schubert: A parameterization of moist convection for general circulation models, *Mon. Weather Rev.*, *120*, 978–1002, doi:10.1175/1520-0493(1992)120<0978:RASAPO>2.0.CO;2.

Murphy, J. M., D. M. H. Sexton, D. N. Barnett, G. S. Jones, M. J. Webb, M. Collins, and D. A. Staniforth (2004), Quantification of modeling uncertainties in a large ensemble of climate change simulations, *Nature*, *430*, 768–772, doi:10.1038/nature02771.

Neale, R., J. H. Richter, and M. Jochum (2008), The impact of convection on ENSO: From a delayed oscillator to a series of events, *J. Clim.*, *21*, 5904–5924, doi:10.1175/2008JCLI2244.1.

Nitta, T. (1978), A diagnostic study of interaction of cumulus updrafts and downdrafts with large-scale motions in GATE, *J. Meteorol. Soc. Jpn.*, *56*, 232–241.

Pacanowski, R. C., and S. M. Griffies (1998), *MOM3.0 Manual*, Geophys. Fluid Dyn. Lab., Natl. Oceanic and Atmos. Admin., Princeton, N. J.

Palmer, T. N. (2001), A nonlinear dynamical perspective on model error: A proposal for nonlocal stochastic-dynamic parameterization in weather and climate prediction models, *Q. J. R. Meteorol. Soc.*, *127*, 279–304.

Palmer, T. N., G. J. Shutts, R. Hagedorn, F. J. Doblas-Reyes, T. Jung, and M. Leutbecher (2005), Representing model uncertainty in weather and climate prediction, *Annu. Rev. Earth Planet. Sci.*, *33*, 163–193, doi:10.1146/annurev.earth.33.092203.122552.

Parthasarathy, B., et al. (1994), All-India monthly and seasonal rainfall series: 1871–1993, *Theor. Appl. Climatol.*, *49*, 217–224, doi:10.1007/BF00867461.

Rajeevan, M., J. Bhate, J. D. Kale, and B. Lal (2006), High resolution daily gridded rainfall data for the Indian region: Analysis of break and active monsoon spells, *Curr. Sci.*, *91*, 296–306.

Rayner, N. A., D. E. Parker, E. B. Horton, C. K. Folland, L. V. Alexander, D. P. Rowell, E. C. Kent, and A. Kaplan (2003), Global analyses of sea surface temperature, sea ice and night marine air temperature since the late nineteenth century, *J. Geophys. Res.*, *108*(D14), 4407, doi:10.1029/2002JD002670.

Redi, M. H. (1982), Oceanic isopycnal mixing by coordinate rotate, *J. Phys. Oceanogr.*, *11*, 1443–1451.

Rienecker, M. M., et al. (2008), The GEOS-5 data assimilation system—Documentation of versions 5.0.1, 5.1.0, and 5.2.0, *NASA Tech. Rep., TM-2008-104606*, vol. , 27, 118 pp. (Available at http://gmao.gsfc.nasa.gov/pubs/docs/GEOS5_104606-Vol27.pdf)

Rodwell, M. J., and T. N. Palmer (2007), Using numerical weather prediction to assess climate models, *Q. J. R. Meteorol. Soc.*, *133*, 129–146, doi:10.1002/qj.23.

Saha, S., et al. (2006), The climate forecast system at NCEP, *J. Clim.*, *19*, 3483–3517, doi:10.1175/JCLI3812.1.

Smagorinsky, J. (1963), General circulation experiments with the primitive equations: I. The basic experiment, *Mon. Weather Rev.*, *91*, 99–164, doi:10.1175/1520-0493(1963)091<0099:GCEWTP>2.3.CO;2.

Sud, Y. C., and A. Molod (1988), The roles of dry convection, cloud-radiation feedback processes and the influence of recent improvements in the parameterization of convection in the GLA GCM, *Mon. Weather Rev.*, *116*, 2366–2387, doi:10.1175/1520-0493(1988)116<2366:TRODCC>2.0.CO;2.

Sud, Y. C., and G. K. Walker (1993), A rain evaporation and downdraft parameterization to complement a cumulus updraft scheme and its evaluation using GATE data, *Mon. Weather Rev.*, *121*, 3019–3039, doi:10.1175/1520-0493(1993)121<3019:AREADP>2.0.CO;2.

Webster, P. J., and S. Yang (1992), Monsoon and ENSO: Selective interactive systems, *Q. J. R. Meteorol. Soc.*, *118*, 877–926, doi:10.1002/qj.49711850705.

Wittenberg, A. T., A. Rosati, N. C. Lau, and J. J. Ploshay (2006), GFDL's CM2 global coupled climate models. Part III: Tropical Pacific climate and ENSO, *J. Clim.*, *19*, 698–722, doi:10.1175/JCLI3631.1.

Wu, R., and B. P. Kirtman (2006), On the impacts of the Indian summer monsoon on ENSO in a coupled GCM, *Q. J. R. Meteorol. Soc.*, *129*, 3439–3468.

Xie, P., and P. Arkin (1996), Analysis of global monthly precipitation using gauge observations, satellite estimates and numerical model predictions, *J. Clim.*, *9*, 840–858, doi:10.1175/1520-0442(1996)009<0840:AOGMPU>2.0.CO;2.

Xue, Y. K., F. J. Zeng, and C. A. Schlosser (1996), SSiB and its sensitivity to soil properties—A case study using HAPEX-Mobilhy data, *Global Planet. Change*, *13*, 183–194, doi:10.1016/0921-8181(95)00045-3.

Zhang, G. J., and N. A. McFarlane (1995), Sensitivity of climate simulations to the parameterization of cumulus convection in the Canadian Climate Center general circulation model, *Atmos. Ocean*, *33*, 407–446.

Zhang, G. J., and M. Mu (2005), Effects of modifications to the Zhang-McFarlane convection parameterization on the simulation of the tropical precipitation in the National Center for Atmospheric Research Community Climate Model, version 3, *J. Geophys. Res.*, *110*, D09109, doi:10.1029/2004JD005617.

Zhang, G. J., and H. Wang (2006), Toward mitigating the double ITCZ problem in NCAR CCSM3, *Geophys. Res. Lett.*, *33*, L06709, doi:10.1029/2005GL025229.

V. Misra, Department of Meteorology, Florida State University, Tallahassee, FL 32306, USA. (vmisra@fsu.edu)